

Enhanced cadmium (II) adsorption via calcium alginate encapsulation of HPMBP in heavy metal remediation

Ane Nurjanah¹ , Sonita A.P. Siboro² , Roni Sujarwadi² , Renaldi Malay² , Putri Ramadhani¹ ,
Asep Nurohmat Majalis¹ , Rusnadi Rusnadi³ , Muhammad Bachri Amran³ 

¹Research Center for Chemistry BRIN, KST BJ. Habibie, Building 452, South Tangerang, Banten 15314, Indonesia

² Research Center for Polymer Technology BRIN, KST BJ. Habibie, Building 460, South Tangerang, Banten 15314, Indonesia

³Department of Chemistry, Faculty of Mathematics and Natural Science, Institute Technology Bandung, Jl. Ganesha No. 10, Bandung 40132, Indonesia

 Corresponding author: anen001@brin.go.id; ORCID: <https://orcid.org/0009-0009-6763-8344>

Received: 10 January 2025; Revised: 16 June 2025; accepted: 12 August 2025

ABSTRACT

Heavy metal contamination from industrial activities poses serious environmental and health risks, particularly from cadmium (Cd), and the removal through adsorption using calcium alginate encapsulated with 1-phenyl-3-methyl-4-benzoyl-5-pyrazolone (HPMBP) offers a promising solution. This study aims to improve Cd(II) ion adsorption by encapsulating HPMBP in calcium alginate beads and assess its effectiveness in contaminated water remediation. HPMBP was synthesized and encapsulated in calcium alginate beads to produce Ca-alginate-HPMBP microcapsules, characterized using FTIR, proton nuclear magnetic resonance (¹H NMR), and Scanning Electron Microscopy (SEM) analysis. Adsorption experiments evaluated pH, contact time, initial Cd(II) concentration, and adsorbent mass effects. Desorption cycles were also tested to evaluate reusability, and environmental samples were examined to assess practical application. Optimal adsorption was achieved at pH 6, with Ca-alginate-HPMBP showing enhanced adsorption capacity (94.34 mg/g) compared to Ca-alginate alone (9.66 mg/g). Adsorption equilibrium was reached within five hours. Higher initial Cd(II) concentrations improved adsorption efficiency, following a Langmuir isotherm model. The material demonstrated high recovery rates in desorption cycles, and field tests with environmental samples showed a Cd(II) recovery rate of 101.89%. Encapsulation of HPMBP in calcium alginate enhances Cd(II) ion adsorption, providing an efficient, reusable adsorbent for heavy metal remediation in contaminated water sources, supporting sustainable solutions for water contamination challenges.

Keywords: Adsorption, calcium alginate, 1-phenyl-3-methyl-4-benzoyl-5-pyrazolone, encapsulation, microcapsules

INTRODUCTION

Data from The United Nations Children's Fund (UNICEF) indicates that 2.2 billion people lack access to clean drinking water [1]. A cause to this crisis is heavy metal contamination, a consequence of intensifying industrial activities that adversely affect both human and environmental health [2]. Heavy metals such as lead, thallium, cadmium, and antimony are commonly released into ecosystems from industrial processes, where they accumulate in soil and water, causing toxicological threats. These metals are non-biodegradable and enter the food chain

through water sources, leading to adverse effects such as carcinogenicity, mutagenicity, and teratogenicity, depending on exposure levels and affected species [3]. The solubility in aquatic environments increase the bioavailability, increasing health risks for populations in industrial zones. Among these toxic metals, cadmium stands out due to its widespread industrial use and significant health risks. Cadmium is a corrosion-resistant, non-flammable metal widely utilized in batteries, polyvinyl chloride (PVC) products, and color pigments [4]. It is released into the environment through activities such as fossil fuel combustion, waste

incineration, and industrial discharges, persisting in air, soil, and water systems. Once absorbed, cadmium accumulates in vital organs such as the kidneys and liver and has been classified as a Group 1 human carcinogen by the International Agency for Research on Cancer (IARC) [5]. Its mobility in aquatic ecosystems highlights the need for effective remediation methods to protect public health and the environment.

Current efforts to mitigate heavy metal contamination in water have focused on efficient removal technologies. Regulatory bodies like the United States Environmental Protection Agency (US EPA) and the World Health Organization (WHO) have established stringent permissible limits for heavy metals in wastewater, emphasizing the urgency for cost-effective and sustainable solutions [6]. Conventional methods such as reverse osmosis and nanofiltration have shown promise but are often limited by high operational costs and energy requirements. In contrast, adsorption is recognized as an economical and highly effective technique for heavy metal removal [2]. Research has explored the use of natural adsorbents like chitosan, cellulose, and alginate due to the biodegradability and modifiability for enhanced adsorptive performance [7]. Chitosan, derived from chitin, cellulose from plant cell walls, and alginate from brown algae, have been functionalized into nanoadsorbents for various applications. Alginate, in particular, has demonstrated the ability in forming calcium alginate beads, which are effective in adsorbing cadmium ions from aqueous solutions [7]. Kwiatkowska-Marks and Wojcik has found the efficacy of calcium alginate beads for cadmium ion removal [8]. The current study is different from previous studies that utilized alginate with various modifiers such as montmorillonite [9], EDTA [10], or algae [11]. This research integrates HPMBP that can improve the adsorption capacity. The reported capacity of 94.34 mg/g surpasses that of comparable systems like calcium alginate-EDTA at 0.0301 mg/g [10], and algae-modified beads with up to 181.0 mg/g [11]. Additionally, the encapsulation approach not only ensures high adsorption efficiency but also enhances the material's stability, addressing limitations such as degradation seen in other adsorbents [11]. A novel feature of this study is its comprehensive evaluation of the adsorbent's performance, including tests on real environmental samples. The system demonstrated an impressive Cd(II) recovery rate of 101.89%, showing its potential for practical application, whereas previous work largely remained under laboratory conditions [2, 9]. By optimizing key parameters (peak performance at pH 6) and fitting data to the Langmuir isotherm model [12], and integrating HPMBP encapsulation, this study offers an effective remediation approach. Importantly, the material also maintained high recovery rates over multiple desorption cycles, overcoming the performance degradation that restricted earlier systems [7].

Encapsulation of HPMBP in calcium alginate beads was selected in this study because HPMBP is a classic β -diketonate chelating agent renowned for its high affinity and selectivity toward divalent metal ions, including Cd(II) [13]. Unlike covalent functionalization methods, encapsulation within a Ca-alginate matrix requires no organic solvents and proceeds under mild, aqueous conditions, making it both economically attractive and environmentally benign [14]. In this configuration, calcium alginate provides a mechanically robust, porous egg-box scaffold that physically entraps HPMBP molecules while preserving their chelating functionality. The primary purpose of encapsulating HPMBP is to combine the ligand's strong coordination chemistry of bidentate carbonyl and hydroxyl donor sites that form stable five-membered chelate rings with Cd²⁺ with the facile separation and reusability of alginate beads. This approach is expected to enhance adsorption capacity, selectivity, and cycletocycle stability compared to unmodified alginate or solventextracted systems [15]. These innovations collectively establish the study's contribution as a step forward in the development of sustainable, efficient, and reusable adsorbents for heavy metal remediation [11]. Based on these advancements, this study aims to improve the adsorptive performance of alginate by encapsulating HPMBP (2-Hydroxy-1-(2-hydroxyphenyl)ethanone oxime) in calcium alginate to create HPMBP-loaded beads. This novel approach is expected to improve cadmium removal efficiency from contaminated water, contributing to the development of more sustainable and effective heavy metal remediation strategies.

EXPERIMENTAL

Materials: The materials used in this study include 1,4-dioxane (99.8%, Sigma-Aldrich), calcium hydroxide (Ca(OH)₂, 95%, Sigma-Aldrich), benzoyl chloride (99%, Sigma-Aldrich), 1-phenyl-3-methyl-5-pyrazolone (PMP, 99%, Sigma-Aldrich) sodium alginate (low viscosity, Sigma-Aldrich), calcium chloride (CaCl₂, 97%, Sigma-Aldrich), cadmium(II) standard solution (Cd(II), 1000 ppm, Merck), copper(II) standard solution (Cu(II), 1000 ppm, Merck), lead(II) standard solution (Pb(II), 1000 ppm, Merck), zinc(II) standard solution (Zn(II), 1000 ppm, Merck), nitric acid (65%, Merck), and deionized water (Milli-Q, Millipore). All chemicals were used as received without further purification.

The chemical structure and purity of the synthesized HPMBP ligand and its encapsulation within calcium alginate beads were confirmed by FTIR spectroscopy and NMR, while the physical morphology and uniformity of the microcapsules were evaluated by optical microscopy and SEM. In FTIR spectra, characteristic β -diketonate C=O stretches, aromatic C–H vibrations, and shifts in alginate's –OH and –COO⁻ bands upon ligand incorporation were identified. ¹H NMR provided chemical shift assignments and integrals for the pyrazolone ring, methyl substituent, and phenyl

protons, confirming the ligand's structure and purity. Optical microscopy enabled rapid quantification of bead size distribution and sphericity from bright-field images, while high-resolution SEM revealed the surface and cross-sectional architecture of the alginate network, including the smooth, homogeneous matrix of plain Ca-alginate beads and the subtle undulations introduced by HPMBP encapsulation.

Synthesis and characterization of HPMBP: The synthesis of HPMBP was performed using a modified Jensen method [16]. Initially, 1-phenyl-3-methyl-5-pyrazolone (PMP) was dissolved in 1,4-dioxane at 45 °C for 20 minutes, followed by the gradual addition of calcium hydroxide at 60 °C, acting as a catalyst. Benzoyl chloride was then slowly introduced to the reaction mixture, which was maintained at 100 °C for two hours. After cooling, 2 M hydrochloric acid was added, resulting in the precipitation of a brown solid. This precipitate was filtered, washed with deionized water and ethanol, and then vacuum-dried. The resulting HPMBP was confirmed through melting point analysis and characterized by FTIR, ¹H NMR, ¹³C NMR, and mass spectrometry, identifying its structure and functional groups.

Preparation of Ca-alginate and Ca-alginate-HPMBP microcapsules: Ca-alginate and Ca-alginate-HPMBP microcapsules were synthesized by dissolving sodium alginate in water at concentrations of 1%, 2%, and 3% to evaluate their mechanical stability and shape. The 2% concentration was identified as optimal due to its superior spherical shape and structural integrity. For the Ca-alginate-HPMBP microcapsules, HPMBP was dispersed uniformly into the sodium alginate solution before being added to a calcium chloride solution, forming yellow microcapsules with diameters of approximately 2 mm. Morphological analysis using optical microscopy and SEM indicated a homogenous structure for Ca-alginate and surface irregularities for Ca-alginate-HPMBP, attributed to the HPMBP encapsulation.

Adsorption experiments for Cd(II) ions: Each adsorbent (0.025 grams) was weighed and placed into plastic bottles, followed by the addition of 25 mL of a 10 ppm Cd(II) solution at specific pH levels ranging from 3 to 8. The mixtures were then agitated at 200 rpm and 25 °C for three hours. To quantify Cd(II) adsorption, standard Cd(II) solutions (0.1 to 7.5 ppm) were prepared for calibration. After the adsorption process, the adsorbents were separated by filtration, and the Cd(II) concentration in the filtrate was measured using Atomic Absorption Spectroscopy (AAS). Each adsorbent (0.025 g) was placed in plastic bottles, and 25 mL of a 10 ppm Cd(II) solution at each adsorbent's optimal pH was added. The mixtures were agitated at 200 rpm and 25 °C for varying contact times (50, 100, 150, 200, 250, 300, 420, 540, and 660 minutes). Standard Cd(II) solutions (0.1 to 7.5 ppm) were prepared for calibration. After adsorption, the adsorbents were separated by

filtration, and the Cd(II) concentration in the filtrate was measured using AAS.

Each adsorbent (0.025 g) was weighed and placed into plastic bottles, followed by the addition of 25 mL of Cd(II) solutions at varying concentrations (5, 10, 15, 20, 30, 40, 50, 60 ppm) at each adsorbent's optimal pH. The mixtures were agitated at 200 rpm and 25 °C for five hours. Standard Cd(II) solutions (0.1 to 7.5 ppm) were prepared for calibration. After the adsorption process, the adsorbents were separated by filtration, and the Cd(II) concentration in the filtrate was measured using AAS.

Adsorbent samples of varying masses (0.025, 0.05, 0.075, 0.1, 0.125, and 0.15 g) were prepared and placed in plastic bottles. A 10 ppm Cd(II) solution, adjusted to each adsorbent's optimal pH, was added in a volume of 25 mL. The mixtures were then agitated at 200 rpm and 25 °C for five hours. Standard Cd(II) solutions (0.1 to 7.5 ppm) were prepared for calibration. After the adsorption process, the adsorbents were separated by filtration, and the Cd(II) concentration in the filtrate was measured using AAS.

Mixed metal adsorption: 0.05 g of Ca-alginate 2% and Ca-alginate-HPMBP were each added to 25 mL solutions containing Cd(II) (10 ppm) combined with either Cu(II) (5 ppm), Pb(II), or Zn(II) (5 ppm) at pH 6. The mixtures were agitated on a shaker at 200 rpm and 25 °C for five hours. After adsorption, the mixtures were filtered, and the absorbance of the filtrate was measured using AAS to determine metal uptake.

Adsorption and desorption method: 0.5 g of Ca-alginate-HPMBP was placed in a column, and 250 mL of a 1 ppm Cd(II) solution was passed through at a flow rate of approximately 2 mL/min. Every 30 minutes, a 5 mL sample of the filtrate was collected over a period of seven hours. Desorption was then performed by passing 30 mL of 0.1 M HNO₃ through the column, collecting 5 mL fractions. The absorbance of both the Cd(II) filtrate and the initial solution was measured using AAS. This experiment was repeated three times.

Statistical method environmental sample application: 0.5 g of Ca-alginate-HPMBP was placed in a column, and 250 mL of an environmental sample solution was passed through at a flow rate of approximately 2 mL/min. Every 30 minutes, 5 mL of filtrate was collected over a period of seven hours. Desorption was performed by passing 30 mL of 0.1 M HNO₃ through the column, collecting 5 mL fractions. The same procedure was repeated with an environmental sample solution with 1 ppm Cd(II) in a volume of 250 mL. The absorbance of the filtrate was measured using AAS. This experiment was repeated twice.

Statistical method: The statistical method employed in this study is descriptive statistics, carried out in Excel to analyze the data using measures such as the mean, median, mode, percentage of adsorption, and so on. This form of analysis is able to clearly summarize and explain the results obtained from the measurements in the research.

RESULTS AND DISCUSSION

Schematic and material characterization of alginate–HPMBP binding: Calcium alginate gelation can be described by the egg-box model, in which divalent Ca^{2+} ions chelate between blocks of α -l-guluronate residues on adjacent alginate chains, forming a three-dimensional network (Fig. 1a → 1b). In this structure each Ca^{2+} is coordinated by four carboxylate oxygens from two alginate chains plus water ligands, creating stable junction zones that entrap small molecules within the gel pores [17]. When HPMBP is present during gelation, two interactions occur simultaneously (Fig. 1b → 1c): First, physical entrapment of HPMBP molecules within the forming gel pores, as the eggbox junction zones close around them; Second, coordination of HPMBP's β -diketone motif (the enolic $\text{O}-\text{C}=\text{O}$ chelate) to the same Ca^{2+} crosslinking nodes, via its carbonyl and hydroxyl donor groups, analogous to its known chelation of alkaline earth metals [18]. These dual interactions immobilize HPMBP without covalent modification, preserving its chelating activity toward incoming Cd^{2+} ions.

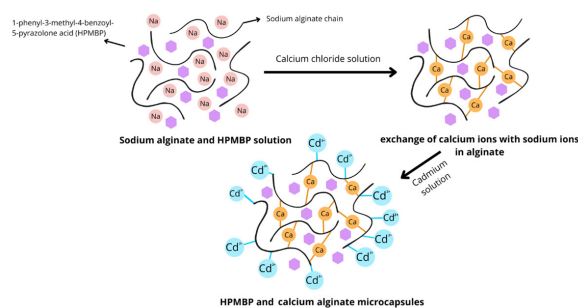


Fig. 1. Schematic of alginate–HPMBP binding: (a) Sodium-alginate chains bearing $-\text{COO}^-$ groups and dispersed HPMBP ligands. (b) Addition of CaCl_2 induces egg-box cross-linking: Ca^{2+} bridges guluronate blocks, trapping HPMBP. (c) Cd^{2+} diffusion into gel and chelation by HPMBP, forming $\text{Cd}-\text{HPMBP}$ complexes within the alginate matrix.

Within the newly formed Ca-alginate gel, HPMBP remains noncovalently immobilized. Its aromatic β -diketonate moiety engages in hydrophobic interactions with less polar microdomains of the gel, an effect analogous to that observed in hydrophobically modified alginate systems used for protein delivery [19]. At the same time, hydrogen bonds form between the carbonyl oxygen of HPMBP and the hydroxyl groups of the alginate backbone, as demonstrated in FTIR studies of small molecule loaded alginate beads where $\text{C}=\text{O}$ and $-\text{OH}$ bands shift upon encapsulation [20]. Additional van der Waals forces contribute to the overall retention of HPMBP within the gel pores, consistent with the weak dipoleinduced interactions known to stabilize guest molecules in polysaccharide hydrogels [21].

In this study, the synthesis of HPMBP was performed using the Jensen method, which involves a reaction between PMP and benzoyl chloride with calcium hydroxide as a catalyst [16]. The temperature-controlled synthesis progressed from 45 °C (PMP dissolution) to 60 °C (catalyst addition) and finally 100 °C (benzoyl chloride reaction), yielding yellow HPMBP [22]. The final product had a yield of 45.37% with a melting point range of 92 - 94 °C, indicating the enol form of HPMBP due to its intramolecular hydrogen bonding, consistent with Akama's findings comparing keto (120 °C) and enol (92 °C) forms [22]. Structural confirmation via FTIR revealed key functional groups, such as aromatic C-H stretching, C=O vibrations, and pyrazolone ring modes, as shown in Fig. 2. The presence of methyl and carbonyl peaks confirms the molecular structure [13].

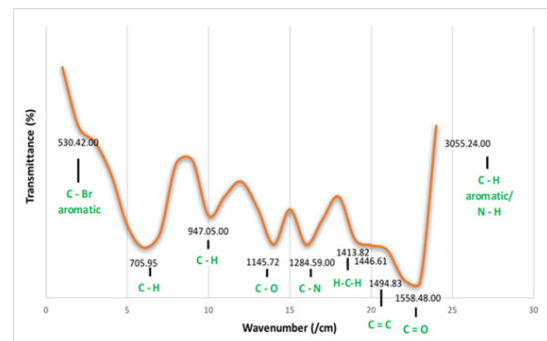


Fig. 2. IR Spectrum of synthesized HPMBP

The ^1H and ^{13}C NMR (Fig. 3, Fig. 4) spectra showed the expected proton and carbon environments typical of β -diketone structures, as demonstrated in other metal complexes using PMBP as a ligand [23]. Meanwhile, the results confirmed a molecular weight of 277.0962 g/mol from the mass spectrum. This finding aligns with the theoretical molecular weight of HPMBP, which is 278.311 g/mol [24].

The downfield portion of the ^1H NMR spectrum (δ 7.00–8.20 ppm) (see Fig. 3) shows that the synthesized HPMBP was obtained as the enolic tautomer, with all five aromatic/heterocyclic protons and the methyl group accounted for, and without detectable impurities. Meanwhile, the ^{13}C NMR spectrum of the synthesized

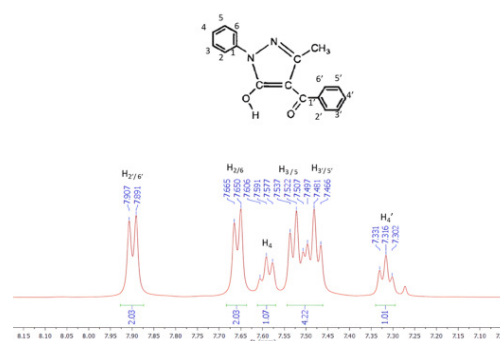


Fig. 3. ^1H NMR analysis of HPMBP

HPMBP displays all of the expected resonances for its methyl, aromatic, heterocyclic and carbonyl carbons (Fig. 4). The result confirming the presence of both the β -diketone and aromatic ketone functionalities in the product.

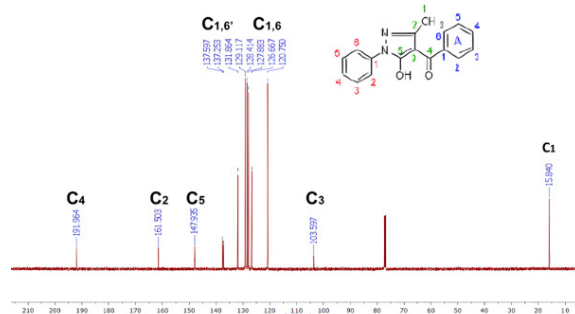


Fig. 4. ^{13}C NMR spectrum of synthesized HPMBP

Preparation of Ca-alginate and Ca-alginate-HPMBP microcapsules:

The synthesis of Ca-alginate and Ca-alginate-HPMBP microcapsules represents an approach to creating effective adsorbents for heavy metal ions. These microcapsules use the unique properties of calcium alginate, a biopolymer known for its stability, biocompatibility, and efficiency in ion adsorption, particularly when combined with other functional agents such as HPMBP [9]. The Ca-alginate microcapsules were synthesized at 1%, 2%, and 3% concentrations, with 2% yielding the optimal spherical shape and mechanical stability (Fig. 5), consistent with previous findings that 2% alginate concentration offers the best balance of these characteristics [25]. Lower concentrations (1%) yielded less rounded shapes, while higher concentrations (3%) enhanced rounding but affected stability. This concentration-dependent morphology aligns with findings that alginate's binding efficiency with calcium ions is influenced by gelation properties, providing the necessary rigidity for effective heavy metal adsorption [26].

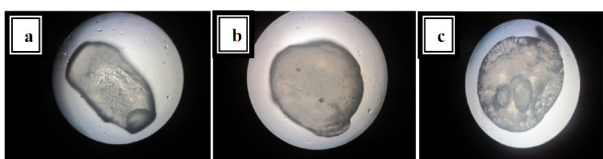


Fig. 5. The form of Ca-alginate microcapsules was observed using an optical microscope (a. Ca-alginate 1%, b. Ca-alginate 2%, c. Ca-alginate 3%)

Ca-alginate-HPMBP microcapsules were developed by dispersing HPMBP into sodium alginate before dripping into calcium chloride using a peristaltic pump, resulting in yellow microcapsules approximately 2 mm in diameter. The color change reflects the interaction of HPMBP with calcium alginate, a common characteristic of functionalized alginate materials [10]. Microscopy and SEM analysis indicated a homogenous morphology for

Ca-alginate, while Ca-alginate-HPMBP showed surface irregularities due to the encapsulated HPMBP (Fig. 6). Microparticle size can be measured using SEM which enables analysis of particle-diameter distributions. In this study, SEM images revealed that the size of calcium-alginate beads was 100 μm , although previous study showed the optimization of less than 100 μm Ca-alginate microcapsules [27]. Meanwhile, the SEM images of the HPMBP-encapsulated calcium-alginate microcapsules show a diameter of approximately 50 μm , which corresponds closely to the 45–50 μm particles obtained by homogenization [28]. This variation in surface morphology results from HPMBP encapsulation, enhances active sites for metal ion interaction due to the additional functional groups introduced by HPMBP [7]. The distinct properties of Ca-alginate and Ca-alginate-HPMBP microcapsules offer promising implementations for selective metal ion removal in contaminated water treatment [7].

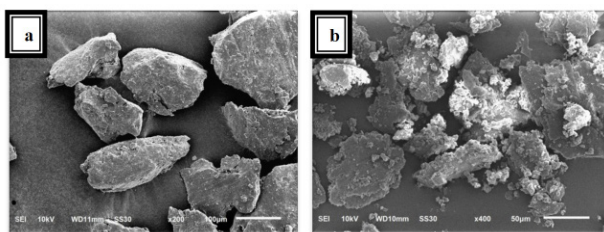


Fig. 6. Surface morphology of microcapsules observed with SEM (a. Ca-alginate, b. Ca-alginate-HPMBP)

Both pure Ca-alginate beads and Ca-alginate-HPMBP microcapsules derive their basic three dimensional egg-box network from Ca^{2+} crosslinking of alginate chains [27]. However, SEM micrographs show that incorporation of the HPMBP ligand notably alters the bead surface. Unmodified Ca-alginate beads exhibit a relatively smooth, continuous exterior, indicative of uniform gelation and minimal phase separation during crosslinking [29]. In contrast, the Ca-alginate-HPMBP microcapsules display pronounced undulations or waves across their surface, together with shallow cavities and nodular features where HPMBP molecules are physically entrapped or adsorbed. In practical terms, the wrinkled, cavity-rich surface of Ca-alginate-HPMBP not only confirms successful encapsulation of HPMBP but also shows its enhanced adsorption performance and selectivity toward Cd(II). The smooth morphology of Ca-alginate, by contrast, reflects a homogeneous gel network without functional ligand domains, explaining its relatively poor heavy metal binding.

Encapsulation efficiency and content of HPMBP in the Ca-alginate: Encapsulation efficiency was determined by first establishing the optimal alginate matrix. Plain Ca-alginate beads prepared at 1, 2, and 3% (w/v) alginate (See Fig. 5) were compared under identical peristaltic pump dripping conditions. Bead roundness, as viewed by optical microscopy, improved

markedly from the 1% to the 2% formulation and plateaued at 3 % (Table 1), indicating that 2% alginate provides the best balance of viscosity and gel strength for uniform bead formation, as shown in previous study [30]. Using the 2% Ca-alginate standard, HPMBP ligand (1 g per batch) was dispersed into the alginate solution and gelled in 0.2 M CaCl_2 . The resulting Ca-alginate-HPMBP beads retained the same spherical morphology, with a slight surface waviness attributable to the entrapped aromatic ligand domains [31].

Cd(II) binding mechanism in Ca-alginate-HPMBP microcapsules: When Ca-alginate HPMBP microcapsules are exposed to a Cd(II) containing

Table 1. Encapsulation efficiency and content of HPMBP in the Ca-alginate

Microcapsule	Concentration	Shape
Ca-alginate 1%	Low	Poorly round
Ca-alginate 2%	Medium	Round
Ca-alginate 2%	High	Round

solution, the Cd^{2+} ions first diffuse through the porous egg-box network of the calcium alginate gel, driven by concentration gradients and aided by the gel's high-water content and interconnected pores [32]. Once inside the gel matrix, Cd^{2+} encounters immobilized HPMBP ligands. HPMBP, a β -diketonate chelator, presents two carbonyl oxygens and an enolic hydroxyl that act as bidentate donor sites, forming a five-membered chelate ring upon coordination to a metal center [33]. The coordination of Cd^{2+} by HPMBP proceeds via donation of lonepair electrons from the ligand's carbonyl oxygens into vacant orbitals on the Cd(II) ion, creating a stable $[\text{Cd}(\text{HPMBP})_2]$ complex within the gel pores. Spectroscopic studies of analogous acylpyrazolone complexes confirm that Cd(II) forms octahedral or pentagonalbipyramidal geometries with β -diketonate ligands, with characteristic shifts in C=O and C=C vibrational bands upon metal binding [18]. Although the alginate network contains carboxylate groups capable of weak electrostatic interaction with Cd^{2+} , the primary binding sites are the HPMBP ligands. Alginate's role is structural, providing the scaffold that localizes and orients HPMBP for optimal chelation [34]. Ionexchange between incoming Cd^{2+} and the gel's Ca^{2+} crosslinks contributes minimally to overall uptake, as demonstrated by comparative elemental analysis of released Ca^{2+} during adsorption [35]. After complexation, the neutral or slightly positive $[\text{Cd}(\text{HPMBP})_2]$ remain trapped within the egg-box matrix, preventing leaching under neutral to mildly acidic conditions. This high retention is confirmed by desorption tests showing 95% recovery under strong acid (0.1 M HNO_3), which protonates ligand donors and disrupts the chelate [36]. The combined diffusionchelation mechanism thus yields both high capacity and selectivity for Cd(II),

outperforming unmodified alginate beads by an order of magnitude in adsorption capacity [33].

Optimal conditions for Cd(II) adsorption by Ca-alginate and Ca-alginate-HPMBP microcapsules:

The adsorption of Cd(II) ions by Ca-alginate and Ca-alginate-HPMBP microcapsules is highly pH-dependent, with optimal adsorption observed at pH 6. At this pH, Ca-alginate-HPMBP microcapsules achieved a maximum adsorption capacity of 94.34 mg/g, while Ca-alginate microcapsules reached 9.66 mg/g. This difference highlights the enhanced adsorption efficiency of Ca-alginate-HPMBP due to the additional functional groups provided by HPMBP, which facilitate stronger binding interactions with Cd(II) ions [34]. The increase in pH induces more negative charges on the microcapsules, which enhances electrostatic attraction between the negatively charged functional groups and the positively charged Cd(II) ions, thereby boosting adsorption efficiency. However, as the pH exceeds 7, the efficiency decreases due to the formation of $\text{Cd}(\text{OH})_2$ precipitates, which interfere with the adsorption process by reducing the availability of free Cd(II) ions for interaction with the microcapsules. This observation aligns with prior studies on alginate-based adsorbents, which show that the optimal pH range avoids conditions where metal hydroxides are likely to form, thus maintaining the ion-exchange and electrostatic interactions crucial for effective adsorption [26].

The study on contact time indicated that adsorption equilibrium was achieved after 5 hours, with adsorption capacities stabilizing at 9.16 mg/g for Ca-alginate and 9.30 mg/g for Ca-alginate-HPMBP. The plateau effect suggests a saturation of active adsorption sites on the microcapsules' surface. This "plateau" effect aligns with other findings where extended contact times contribute to reaching maximum adsorption capacity as the number of available binding sites decreases, suggesting that the adsorption mechanism is regulated by pseudo-second-order kinetics, a model commonly applicable to studies on heavy metal ion adsorption [12]. As observed in the current study, rapid initial adsorption followed by a slower rate until equilibrium suggests that the Ca-alginate beads have a high affinity for Cd(II) ions, which is a typical behavior of biosorbents with high porosity and surface area, such as alginate-based materials [11]. The plateau achieved after a certain period indicates the completion of ion exchange and surface complexation reactions [26]. Furthermore, the marginal increase in capacity observed with Ca-alginate-HPMBP over Ca-alginate alone highlights the slight improvement in binding sites offered by the HPMBP modification. This modification enhances the material's chelation ability, slightly increasing Cd(II) uptake compared to unmodified Ca-alginate. These findings are consistent with research indicating that modified alginates often present higher adsorption capacities due to improved mechanical stability and additional functional groups that facilitate metal ion

binding [37].

The adsorption efficiency improved with increased Cd(II) concentrations, peaking at 25 ppm with adsorption capacities of 23.23 mg/g for Ca-alginate and 23.25 mg/g for Ca-alginate-HPMBP. This indicates the microcapsules' effectiveness at higher metal concentrations, making them suitable for environments with elevated cadmium contamination. Aligned with this result, Rusnadi (2023) noted that Cd(II) adsorption onto calcium alginate beads demonstrated enhanced efficiency with higher concentrations, following a Langmuir isotherm model, which reflects monolayer adsorption onto a homogeneous surface [38]. Similarly, Mahmood *et al.* (2017) indicated that alginate-calcium carbonate composites showed increased adsorption capacity at higher metal concentrations, further supporting this trend [34]. The minor difference in adsorption capacities between Ca-alginate and Ca-alginate-HPMBP indicates that while HPMBP modification slightly improves binding, both types of microcapsules maintain similar adsorption capabilities, especially at elevated metal concentrations. This suggests that Ca-alginate alone can be quite effective, but modifications with chelating agents like HPMBP may offer incremental improvements in certain conditions [39]. This efficiency in Cd(II) removal highlights the potential of these materials in treating industrial wastewater, as noted by Elwakeel *et al.* (2022), who emphasized the cost-effectiveness and environmental sustainability of alginate-based adsorbents for heavy metals [26].

The study found that increasing adsorbent mass led to greater Cd(II) uptake, reaching an optimal capacity of 8.63 mg/g for Ca-alginate and 8.78 mg/g for Ca-alginate-HPMBP at 0.05 g. Further increases in mass did not significantly impact adsorption, as active sites were fully saturated at this threshold [12]. Additionally, Yantyana *et al.* (2018) highlighted the effect of adsorbent mass on lead ion uptake, illustrating that increasing adsorbent mass enhanced adsorption until a saturation point, a pattern consistent with the behavior observed in this study with Cd(II) ions [37]. The findings align with the Langmuir adsorption model, where a plateau indicates the saturation of adsorption sites as seen in similar Ca-alginate-based adsorbents. The study thus concludes that while increasing adsorbent mass generally improves metal ion removal efficiency, there is a threshold beyond which additional adsorbent mass does not lead to higher adsorption due to site saturation [12].

Adsorption isotherms: The adsorption isotherm models revealed that Cd(II) adsorption onto both microcapsules followed the Langmuir model, indicating monolayer coverage on a homogenous surface. This suggests a uniform distribution of adsorption sites, with each site binding to a single Cd(II) ion. This homogeneity supports the Ca-alginate and Ca-alginate-HPMBP microcapsules' suitability for single-layer ion

adsorption applications. Sarkar *et al.* (2017) emphasize that this single-layer adsorption is typical for Ca-alginate systems, as they often exhibit consistent interaction with Cd(II) ions due to uniform surface properties in aqueous solutions [40]. Rusnadi *et al.* (2023) reveals that the Langmuir isotherm fits well with Ca-alginate composites modified to enhance adsorption [12]. These modified materials show greater affinity for Cd(II), and the adsorption capacities align with a pseudo-second-order kinetic model, supporting chemisorption where Cd(II) [12] ions bind with active sites on the Ca-alginate matrix, enhancing removal efficiency [12]. The Freundlich isotherm model, applied to assess the adsorption behavior across different concentrations, showed a poorer fit in this study compared to the Langmuir model. This outcome is consistent with findings from Mahmood *et al.* (2017), where the Ca-alginate composites exhibited a preference for monolayer adsorption, reinforcing that these materials are more effective in homogeneous, single-ion conditions rather than multilayer adsorption settings [34]. The uniform surface structure and consistent ion binding, as noted by Zhou *et al.* (2018), further affirm that Ca-alginate and its composites are well-suited for controlled and efficient Cd(II) adsorption applications in water treatment [41].

Adsorption kinetics: The kinetic showed that Cd(II) adsorption follows both pseudo-first-order and pseudo-second-order models. In the pseudo-first-order model (Fig. 7), the rate of Cd(II) adsorption is proportional to the difference between the amount adsorbed at equilibrium and at any given time, implying that the process is primarily based on single-site interactions. The linearity in the graph for Ca-alginate and Ca-alginate-HPMBP indicates high consistency with the pseudo-first-order model, with regression coefficients (R^2) of 0.9975 and 0.999, respectively, suggesting a strong fit to this model. This is consistent with findings from studies where alginate-based adsorbents follow similar kinetic behavior due to their availability of binding sites that reduce over time as the adsorbent becomes saturated. In contrast, Fig. 8 displays the pseudo-second-order kinetic model, which suggests that the rate of adsorption is dependent on the square of the number of unoccupied sites. This model aligns with the observed data for both types of microcapsules, achieving (R^2) values of 0.9962 for Ca-alginate and 0.9987 for Ca-alginate-HPMBP. This high correlation supports the hypothesis that the adsorption of Cd(II) onto these materials involve chemisorption, a mechanism that includes electron sharing or exchange between the Cd(II) ions and the active sites on the adsorbent surface, which is common in alginate-based biosorbents [11, 12]. These findings align with other studies on similar materials, where Cd(II) adsorption often follows pseudo-second-order kinetics due to interactions with the carboxyl and hydroxyl functional groups present in alginate and modified alginate composites. The enhanced performance of Ca-alginate-

HPMBP microcapsules compared to Ca-alginate alone suggests that the HPMBP modification increases the availability of active sites and improves adsorption efficiency [39].

Mixed metal adsorption: The study on mixed metal adsorption using calcium alginate (Ca-alginate) and

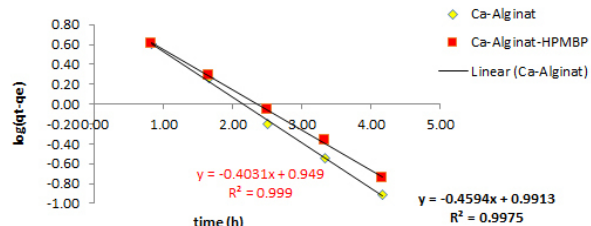


Fig. 7. Pseudo-first-order reaction curve of lagergren by Ca-alginate and Ca-alginate-HPMBP microcapsules

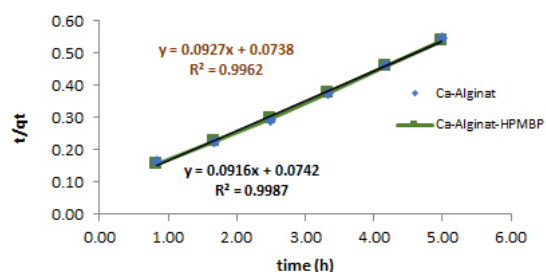


Fig. 8. Pseudo-second-order reaction curve by Ca-alginate and Ca-alginate-HPMBP microcapsules

its modified version with hydroxyl phosphono methyl butanoic acid (Ca-alginate-HPMBP) explores selective adsorption properties in binary metal systems of Cu(II), Zn(II), and Pb(II). Findings reveal that Ca-alginate-HPMBP has greater selectivity for Pb(II) and Cu(II) over Cd(II), attributed to differences in the ionic radii that affect binding affinity. The enhanced selectivity is evident through the distribution ratios and selectivity

to their improved structural framework, which allowed for higher selectivity and capacity [25]. Similarly, studies using calcium alginate-based materials have demonstrated that their porous nature and chemical stability provide an effective framework for selective ion adsorption, which is beneficial for environmental applications in heavy metal removal. In addition, modifications like the one seen with HPMBP can optimize the performance of Ca-alginate by tuning its binding affinity through ionic radius compatibility, a principle similarly noted in the adsorption characteristics of other Ca-alginate modifications [42]. These modifications aid in tailoring the adsorption behavior of alginate-based materials for specific ions, providing insight into their selective applications in wastewater treatment and environmental remediation [42].

Adsorption and desorption cycles: The reusability of Ca-alginate-HPMBP was tested through repeated adsorption-desorption cycles, achieving over 90% efficiency in the recovery of Cd(II) ions across three cycles (Table 3). The process involved desorption with 1 M HNO₃, maintaining high recovery rates and stable adsorption capacity over cycles. Similar studies have shown that the reusability and efficiency of adsorbents in heavy metal recovery depend on the adsorbent material, desorption solution, and operational conditions. Research on Ca-alginate immobilized *Providencia vermicola* for Pd(II) ion recovery showed high adsorption capacity and stability across multiple cycles, using 0.1 M HCl for effective desorption [43]. Additionally, β -cyclodextrin derivatives have been used for Pb(II), Cd(II), and Mn(II) adsorption, achieving good reusability in regeneration experiments, emphasizing the suitability of modified natural materials for heavy metal adsorption [44]. Ferrihydrite's sponge-like structure has proven effective for Cd(II) adsorption, with desorption rates influenced by solution pH and metal concentration, showcasing the need for fine-tuned conditions in adsorption-desorption cycles [45].

Table 2. Results of mixed metal adsorption testing by microcapsules

Microcapsule	D _{Zn}	D _{Cu}	D _{Pb}	α_{Cd-Zn}	α_{Cd-Cu}	α_{Cd-Pb}
Ca-alginate	5.99 \pm 0.11	19.83 \pm 0.61	15.15 \pm 0.08	1.50 \pm 0.06	0.54 \pm 0.04	0.76 \pm 0.04
Ca-alginate-HPMBP	8.84 \pm 0.04	26.78 \pm 0.56	28.35 \pm 0.08	1.15 \pm 0.04	1.04 \pm 0.09	1.08 \pm 0.09

factors, as seen in Table 2, where Ca-alginate-HPMBP consistently shows a higher capacity for adsorbing Pb(II) and Cu(II) in mixed-metal conditions, surpassing the performance of Ca-alginate alone [2]. The basis of this enhanced selectivity in Ca-alginate-HPMBP is its structural modification, which introduces functional groups that engage more effectively with specific metal ions, a property that aligns with findings on composite hydrogels. For example, Lin *et al.* (2021) observed that composite hydrogels involving Ca-alginate with additional components like chitosan and bentonite displayed significant adsorption for heavy metals due

Studies on modified attapulgite demonstrated high Cd(II) adsorption with simple acid regeneration, aligning with the reusability observed in Ca-alginate-HPMBP [46]. Biochar, particularly from soybean roots, has also shown effective Cd(II) adsorption, with temperature-dependent adsorption capacity, highlighting the structural resilience of biochar under repeated cycles [47]. Alginate beads modified with algae demonstrated high Cd(II) removal efficiency due to functional groups like hydroxyl and carboxyl, providing insights into the enhanced performance observed in Ca-alginate-HPMBP for heavy metal recovery [11].

Table 3. Adsorption and desorption cycle by Ca-alginate-HPMBP

Trial No.	Cd(II) Concentration (mg)		% recovery (desorption/adsorption)
	Adsorption	Desorption	
1	0.31	0.32	102.15 ± 3.49
2	0.26	0.24	97.07 ± 3.49
3	0.38	0.36	95.46 ± 3.49

Environmental sample application: In the study examining the environmental application of Ca-alginate-HPMBP microcapsules for cadmium (Cd) remediation, researchers tested these microcapsules on river water from the Cikilai River, which is suspected of being contaminated by industrial cadmium. The microcapsules demonstrated a high recovery rate of 101.89% for Cd(II) ions, underscoring their efficiency in preconcentrating cadmium for easier quantification and detection, as shown in the analysis data from Table 3. The findings align with other research indicating that alginate-based materials, particularly those cross-linked with calcium, are effective adsorbents for heavy metals in contaminated water sources. For instance, alginate

Table 4. Preconcentration results by Ca-alginate-HPMBP on environmental samples

Sample	Amount of Cd(II) Ions (µg)		% recovery
	Before Preconc.	After Preconc.	
Cikilai River Water Sample (Measured Cd(II))	0	1.00	
Sample + Spike (Measured Cd(II) Spike)	13.5	37.1	101.89% ± 0.02
Spike (Cd(II) spike)	35.4	-	

gels have been shown to remove over 95% of cadmium ions when used in high-surface-area formats, such as in a magnetic carbon aerogel [48]. Furthermore, the high recovery rate achieved here with Ca-alginate-HPMBP compares well with other studies on similar biosorbent materials like chitosan and alginate composites, which can also selectively bind Cd ions and effectively extract them from complex environmental matrices [49]. This adsorption efficiency may be attributed to the binding capabilities of calcium alginate, which, when cross-linked with specific chelating agents like HPMBP, facilitates strong ionic and possibly covalent interactions

Table 5. Comparison table between current result with previous studies

Material	Adsorption capacity (mg/g)	Operating conditions	Cost considerations	Advantages	Disadvantages	References
Ca-alginate-HPMBP	94.34	pH 6, equilibrium in 5 hours, Langmuir model	Moderate, scalable encapsulation of HPMBP	High selectivity, reusable, practical for real-world applications, high recovery rate (101.89%)	Initial synthesis of HPMBP requires specific chemicals and controlled conditions	Current Study
Algae-modified alginate beads	181.0	pH-dependent, requires specific algae types	Low, uses sustainable algae sources	Excellent adsorption efficiency, sustainable, eco-friendly	Requires algae immobilization, less practical for industrial scalability	[11]
Alginate-EDTA microcapsules	0.0301	Optimized at 1% sodium alginate, 0.1 M CaCl ₂	Low, easily prepared with common reagents	Simple production process, useful for low cadmium concentrations	Very low adsorption capacity compared to alternatives	[10]
Alginate film (A-F-2%)	84.5	pH 4.5, 150 rpm, 60 mins equilibrium	Low-cost, renewable material	High adsorption efficiency, rapid equilibrium	Lower stability in complex matrices	[9]
Alginate-Chitosan gel films	Pb: 159.74, Cd: 60.98	pH 6.5, adsorption equilibrium in 15 minutes	Moderate, biopolymer films are reusable	High efficiency, short contact time, high reuse potential	Performance drops with repeated cycles for Pb(II), less robust for multi-metal environments	[49]
Alginate-based magnetic nanocomposite beads	Cu: 10.2-43.6, Ni: 15.0-87.3, Cr: 2.67-36.8	Temperature: 25 °C Contact time: 10 min Low pH range: 5.2-6.0	Economic base, MNPs increase cost	High removal, magnetic separation, easy handling	Slower kinetics, complex preparation	[7]
Calcium alginate-PVA beads	33.90	pH 4, contact time 4 hours, Langmuir model	Low cost, alginate from seaweed, scalable	High selectivity, reusable, suitable for cadmium ions	Limited capacity for high Cd(II) concentrations, less effective in multi-metal solutions	[12]
CTS/CA/BT composite hydrogel	Pb ²⁺ : 434.89, Cu ²⁺ : 115.30, Cd ²⁺ : 102.38	pH 5, 25 °C, 10 mg hydrogel, ion concentration: 200–500 mg/L	Low-cost, energy-efficient synthesis	High adsorption capacity, eco-friendly, reusable, Pb ²⁺ selectivity	Reduced efficiency at extreme pH or high competing ion concentrations	[25]
ZnFC/Cyanex 272/Alginate composite beads	Cs ⁺ : 71.7, Co ²⁺ : 34.9	pH 5, 25 °C, adsorbent dose: 0.02 g	Moderate cost, reusable for 3 cycles	High selectivity for Cs ⁺ and Co ²⁺ , reusable, effective with competing ions	Reduced efficiency after multiple cycles	[52]
Alginate-derived starbon®	Cu ²⁺ : 44.8 (2.8 mmol/g)	pH 4.5, pyrolysis temperature: 200–300 °C	Sustainable, low-cost material	High selectivity for Cu ²⁺ , reusable, environmentally friendly	Reduced capacity at higher pyrolysis temperatures	[2]
Soybean root biochar	138.54	pH ~6, 180 min, pyrolysis at 900 °C	Low cost, derived from agricultural waste	High surface area, effective Cd(II) removal	Requires high pyrolysis temperature	[47]

with cadmium ions [50]. Additionally, studies on other biomaterial composites, such as calcium-crosslinked alginate with bacteria for bioremediation purposes, confirm that these materials can maintain their sorptive effectiveness in natural settings and be regenerated for repeated use, adding to their sustainability potential [51]. Thus, the application of Ca-alginate-HPMBP microcapsules for cadmium recovery in natural water samples, as demonstrated in this study, is corroborated by prior research. It suggests that such materials could play an important role in real-world remediation of heavy metal contaminants in aquatic environments [50]. Comprehensive comparison table summarizing the results of the current study and similar materials with details on adsorption capacities, operating conditions, cost considerations, and advantages/disadvantages can be seen in Table 5.

CONCLUSIONS

The encapsulation of HPMBP in calcium alginate has proven to enhance the adsorption capacity for cadmium (Cd(II)) ions, with optimized pH, contact time, and adsorbent mass parameters providing an effectiveness in Cd(II) removal from water sources. The Ca-alginate-HPMBP microcapsules not only demonstrated better adsorption compared to Ca-alginate alone but also showed recovery rates and reusability in desorption cycles, highlighting their potential as a sustainable, cost-effective adsorbent for heavy metal remediation. The success in environmental sample testing further supports the practical application of Ca-alginate-HPMBP for real-world water treatment, offering a solution to address the growing issue of industrial heavy metal contamination in water resources.

LIMITATION AND FUTURE STUDY

The limitation of the present study is that material characterization was confined to SEM imaging. To gain deeper insight into the physicochemical properties governing adsorption performance, future study should include additional surface and structural analyses, such as thermogravimetric analysis (TGA), point of zero charge (pHzpc) determination, X-ray diffraction (XRD), energy-dispersive X-ray spectroscopy (EDS), and X-ray photoelectron spectroscopy (XPS). These complementary techniques will elucidate pore structure, thermal stability, surface charge, crystallinity, elemental composition, and chemical state of the adsorbent, thereby guiding further optimization of Ca-alginate-HPMBP microcapsules for enhanced heavy-metal remediation.

DISCLOSURE STATEMENT

The authors declare that they have no known competing financial interests or personal relationships that could have appeared to influence the work reported in this paper.

DATA AVAILABILITY STATEMENT

The data presented in this study are available on request from the corresponding author.

REFERENCES

1. UNICEF. Drinking Water data.unicef.org/topic/water-and-sanitation/drinking-water, Universal access to safe drinking mainly to women and girls. [Access to drinking water - UNICEF DATA](https://doi.org/10.1002/cssc.202400015)
2. Garland N., Gordon R., McElroy C.R., Parkin A., MacQuarrie D. (2024) Optimising low temperature pyrolysis of mesoporous alginate-derived starbon® for selective heavy metal adsorption. *Chem. Sus. Chem.*, 17, e202400015, 1–9. <https://doi.org/10.1002/cssc.202400015>
3. Dasharathy S., Arjunan S., Maliyur Basavaraju A., Murugasen V., Ramachandran S., et al. (2022) Carcinogenic, and teratogenic effect of heavy metals. *Evidence-based Complementary and Alternative Medicine*, 011953. <https://doi.org/10.1155/2022/8011953>
4. Suhani I., Sahab S., Srivastava V., Singh R P. (2021) Impact of cadmium pollution on food safety and human health. *Curr. Opin. Toxicol.*, 27, 1–7. <https://doi.org/10.1016/j.cotox.2021.04.004>
5. Raad H.F., Pardakhti A., Kalarestaghi H. (2021) Carcinogenic and non-carcinogenic health risk assessment of heavy metals in ground drinking water wells of Bandar Abbas. *Pollution*, 7(2), 395–404. <https://doi.org/10.22059/poll.2021.317359.995>
6. Kinuthia G.K., Ngure V., Beti D., Lugalia R., Wangila A., et al. (2020) Levels of heavy metals in wastewater and soil samples from open drainage channels in Nairobi, Kenya: Community health implication. *Sci. Rep.*, 10(1), 1–13. <https://doi.org/10.1038/s41598-020-65359-5>
7. Russo E., Sgarbossa P., Gelosa S., Copelli S., Sieni E., et al. (2024) Adsorption of heavy metal ions on alginate-based magnetic nanocomposite adsorbent beads. *Materials*, 17(9). <https://doi.org/10.3390/ma17091942>
8. Kwiatkowska-Marks S., Wójcik M. (2014) Removal of cadmium(II) from aqueous solutions by calcium alginate beads. *Separation Science and Technology (Philadelphia)*, 49(14), 2204–2211. <https://doi.org/10.1080/01496395.2014.912223>
9. Pratama B.S., Hambali E., Yani M., Matsue N. (2022) Pemanfaatan film alginat dan alginat/montmorillonite sebagai adsorben Cu(II). *J. Sains Dasar*, 11(2), 70–77. <https://doi.org/10.21831/jsd.v11i2.51544>
10. Pratiwi S.W., Triastuti A., Nurmala Sari R., Pinarti I. (2020) Optimasi pembuatan mikrokapsul kalsium-alginat-EDTA sebagai adsorben untuk logam kadmium. *Jurnal Pijar Mipa*, 15(4), 384–391. <https://doi.org/10.29303/jpm.v15i4.1894>
11. Simonić M. (2024) Algae modified alginate

beads for improved Cd(II) removal from aqueous solutions. *Sustainability (Switzerland)*, **16**(18). <https://doi.org/10.3390/su16188174>

12. Rusnadi R. (2023) Pembuatan dan penggunaan bulir kalsium alginat-PVA (polivinil alkohol) untuk adsorpsi ion Cd(II). *Jurnal Kartika Kimia*, **6**(1), 38–44. <https://doi.org/10.26874/jkk.v6i1.200>

13. Cheng Y.-Z., Tang Y., Yan F. (2014) Synthesis and crystal structure of Pb(II) complex with 1-phenyl-3-methyl-4-benzoyl-5-pyrazolone. *Main Group Metal Chemistry*, **37**(3–4). <https://doi.org/10.1515/mgmc-2014-0005>

14. Zadeike D., Gaizauskaite Z., Basinskiene L., Zvirdauskiene R., Cizekiene D. (2024) Exploring calcium alginate-based gels for encapsulation of lacticaseibacillus paracasei to enhance stability in functional breadmaking. *Gels*, **10**(10), 641. <https://doi.org/10.3390/gels10100641>

15. Demakov P.A. (2023) Properties of aliphatic ligand-based metal–organic frameworks. *Polymers (Basel)*, **15**(13), 2891. <https://doi.org/10.3390/polym15132891>

16. Jensen B.S. (1959) The synthesis of 1-phenyl-3-methyl-4-acyl-pyrazolones-5. *Acta Chem. Scand.*, **13**(8), 1668-1670. <https://doi.org/10.3891/acta.chem.scand.13-1668>

17. Plazinski W. (2011) Molecular basis of calcium binding by polygluronate chains. revising the egg-box model. *J. Comput. Chem.*, **32**(14), 2988-2995. <https://doi.org/10.1002/jcc.21880>

18. Mies T., White A. J.P., Rzepa H.S., Barluzzi L., Devgan M., et al. (2023) Syntheses and characterization of main group, transition metal, lanthanide, and actinide complexes of bidentate acylpyrazolone ligands. *Inorg. Chem.*, **62**(33), 13253–13276. <https://doi.org/10.1021/acs.inorgchem.3c01506>

19. Rastello De Boisseson M., Leonard M., Hubert P., Marchal P., Stequert A., et al. (2004) Physical alginate hydrogels based on hydrophobic or dual hydrophobic/ionic interactions: Bead formation, structure, and stability. *J. Colloid Interface Sci.*, **273**(1), 131–139. <https://doi.org/10.1016/j.jcis.2003.12.064>

20. Helmiyati A.M. (2017) Characterization and properties of sodium alginate from brown algae used as an ecofriendly superabsorbent. *IOP Conf. Ser. Mater. Sci. Eng.*, **188**, 012019. <https://doi.org/10.1088/1757-899X/188/1/012019>

21. Patil R., Das S., Stanley A., Yadav L., Sudhakar A., et al. (2010) Optimized hydrophobic interactions and hydrogen bonding at the target-ligand interface leads the pathways of drug-designing. *PLoS One*, **5**(8), e12029. <https://doi.org/10.1371/journal.pone.0012029>

22. Akama Y., Tong A. (1996) Spectroscopic studies of the keto and enol tautomers of 1-phenyl-3-methyl-4-benzoyl-5-pyrazolone. *Microchemical Journal*, **53**(1), 34–41. <https://doi.org/10.1006/mchj.1996.0006>

23. Zhang L.P., Deng S.E., Wang X.D. (2015) Synthesis and crystal structure of a new 2D supramolecular Cd(II) complex with 1-phenyl-3-methyl-4-benzoyl-5-pyrazolone ligand. *Main Group Metal Chemistry*, **38**(1-2), 37-42. <https://doi.org/10.1515/mgmc-2014-0044>

24. ChemSpider. 1-phenyl-3-methyl-4-benzoyl-5-pyrazolone <https://www.chemspider.com/Chemical-Structure.88169.html>

25. Lin Z., Yang Y., Liang Z., Zeng L., Zhang A. (2021) Preparation of chitosan/calcium alginate/bentonite composite hydrogel and its heavy metal ions adsorption properties. *Polymers (Basel)*, **13**(11). <https://doi.org/10.3390/polym13111891>

26. Elwakeel K.Z., Ahmed M.M., Akhdhar A., Sulaiman M.G.M., Khan Z.A. (2022) Recent advances in alginate-based adsorbents for heavy metal retention from water: A review. *Desalination Water Treat*, **272**, 50-74. <https://doi.org/10.5004/dwt.2022.28834>

27. Anani J., Noby H., Zkria A., Yoshitake T., ElKady M. (2022) Monothetic analysis and response surface methodology optimization of calcium alginate microcapsules characteristics. *Polymers (Basel)*, **14**(4), 709. <https://doi.org/10.3390/polym14040709>

28. Samak Y.O., El Massik M., Coombes A.G.A. (2017) A comparison of aerosolization and homogenization techniques for production of alginate microparticles for delivery of corticosteroids to the colon. *J. Pharm. Sci.*, **106**(1), 208-216. <https://doi.org/10.1016/j.xphs.2016.08.015>

29. Petchsomrit A., Sermkaew N., Wiwattanapatapee R. (2013) Effect of alginate and surfactant on physical properties of oil entrapped alginate bead formulation of curcumin. *Inter. J. Med. Health, Biomed. Bioeng. Pharma. Eng.*, **7**, 864-868. https://www.researchgate.net/publication/259761087_Effect_of_Alginate_and_Surfactant_on_Physical_Properties_of_Oil_Entrapped_Alginate_Bead_Formulation_of_Curcumin

30. Elnashar M.M., Yassin M.A., Abdel Moneim A.E.F., Abdel Bary E.M. (2011) Investigating the unexpected behavior for the release kinetics of brilliant blue encapsulated into calcium alginate beads. *Eurasian Chemico-Technological Journal*, **12**(1), 69-77. <https://doi.org/10.18321/ectj209>

31. Haili H.M., Rusnadi Yulianti S.N. (2023) The Ce3+ metal ion adsorbent based on calcium alginate loaded Fe3O4 (Ca-Alg/Fe3O4). *Inter. J. Appl. Res. Sustain. Sci.*, **1**(4). <https://doi.org/10.59890/ijarss.v1i4.1094>

32. Ben Salem D., Yahiaoui K., Bernardo M., Gatica J.M., Ouakouak A., et al. (2025) Insights into cadmium adsorption characteristics and

mechanisms by new granular alginate hydrogels reinforced with biochar: important role of cation exchange. *J. Environ. Manage.*, **383**, 125407. <https://doi.org/10.1016/j.jenvman.2025.125407>

33. Shukla R. (2002) Solvent extraction of metals with potassium-dihydro-bispyrazolyl-borate. *Talanta*, **57**(4), 633–639. [https://doi.org/10.1016/S0039-9140\(02\)00080-2](https://doi.org/10.1016/S0039-9140(02)00080-2)

34. Mahmood Z., Amin A., Zafar U., Raza M.A., Hafeez I., Akram A. (2017) Adsorption studies of cadmium ions on alginate–calcium carbonate composite beads. *Appl. Water Sci.*, **7**(2), 915-921. <https://doi.org/10.1007/s13201-015-0302-2>

35. Pan L., Wang Z., Yang Q., Huang R. (2018) Efficient removal of lead, copper and cadmium ions from water by a porous calcium alginate/graphene oxide composite aerogel. *Nanomaterials*, **8**(11), 957. <https://doi.org/10.3390/nano8110957>

36. Wang S., Wang Y., Wang X., Sun S., Zhang Y., et al. (2024) Study on adsorption of Cd in solution and soil by modified biochar–calcium alginate hydrogel. *Gels*, **10**(6), 388. <https://doi.org/10.3390/gels10060388>

37. Yantyana I., Amalia V., Fitriyani R. (2018) Adsorpsi ion logam Timbal(II) menggunakan mikrokapsul ca-alginat. *Al-Kimiya*, **5**(1), 17-26. <https://doi.org/10.15575/ak.v5i1.3721>

38. Rusnadi R., Buchari B., Amran M. B., Wahyuningrum D. (2012) Cerium adsorption using 1-phenyl-3-methyl-4-benzoyl- 5-pyrazolone (HPMBP) loaded calcium alginate beads. *Int. J. Eng. Res. Appl.*, **2**(5), 496-499. <https://www.researchgate.net/publication/283976716>

39. Alp Arıcı T., Özcan A.S., Özcan A. (2020) Biosorption characteristics of Cu(II) and Cd(II) ions by modified alginate. *J. Polym. Environ.*, **28**(12), 3221-3234. <https://doi.org/10.1007/s10924-020-01844-2>

40. Sarkar K., Sen K., Lahiri S. (2017) Radiometric analysis of isotherms and thermodynamic parameters for cadmium(II) adsorption from aqueous medium by calcium alginate beads. *J. Radioanal. Nucl. Chem.*, **312**(2), 343-354. <https://doi.org/10.1007/s10967-017-5213-2>

41. Zhou F., Fen, X., Yu J., Jiang X. (2018) High performance of 3D porous graphene/lignin/ sodium alginate composite for adsorption of Cd(II) and Pb(II). *Environ. Sci. Poll. Res.*, **25**(16), 15651-15661. <https://doi.org/10.1007/s11356-018-1733-8>

42. Nită I., Iorgulescu M., Spiroiu M.F., Ghiurea M., Petcu C., et al. (2007) The adsorption of heavy metal ions on porous calcium alginate microparticles. *Analele UniversităŃii din Bucureşti, I*, 59-67.

43. Xie J., Feng N., Wang R., Guo Z., Dong H., et al. (2020) A Reusable biosorbent using Ca-alginate immobilized providencia vermicola for Pd(II) recovery from acidic solution. *Water Air Soil Pollut.*, **231**(2). <https://doi.org/10.1007/s11270-020-4399-z>

44. Zhang M., Zhu L., He C., Xu X., Duan Z., et al. (2019) Adsorption performance and mechanisms of Pb(II), Cd(II), and Mn(II) removal by a β -cyclodextrin derivative. *Environ. Sci. Poll. Res.*, **26**(5), 5094-5110. <https://doi.org/10.1007/s11356-018-3989-4>

45. Liang Y., Tian L., Lu Y., Peng L., Wang P., et al. (2018) Kinetics of Cd(II) adsorption and desorption on ferrihydrite: Experiments and modeling. *Environ. Sci. Process Impacts*, **20**(6), 934-942. <https://doi.org/10.1039/c8em00068a>

46. He Y., Sun X., Zhang P., Wang F., Zhao Z., He C. (2020) Cd(II) adsorption from aqueous solutions using modified attapulgite. *Research on Chemical Intermediates*, **46**(11), 4897-4908. <https://doi.org/10.1007/s11164-020-04201-z>

47. Wang Q., Cui P., Yang Q., Chen L., Wang W., et al. (2021) Analysis of the Cd(II) adsorption performance and mechanisms by soybean root biochar: Effect of pyrolysis temperatures. *Bull. Environ. Contam. Toxicol.*, **107**(3), 553-558. <https://doi.org/10.1007/s00128-021-03235-2>

48. Li Y., Zhou M., Waterhouse G.I.N., Sun J., Shi W., et al. (2021) Efficient removal of cadmium ions from water by adsorption on a magnetic carbon aerogel. *Environ. Sci. Poll. Res.*, **28**(5), 5149-5157. <https://doi.org/10.1007/s11356-020-10859-0>

49. Moreno-Rivas S.C., Ibarra-Gutiérrez M.J., Fernández-Quiroz D., Lucero-Acuña A., Burgara-Estrella A.J., et al. (2024) pH-responsive alginate/chitosan gel films: An alternative for removing cadmium and lead from water. *Gels*, **10**(10). <https://doi.org/10.3390/gels10100669>

50. Hamid N.H.A., Rushdan A.I., Nordin A.H., Husna S.M.N., Faiz Norrrahim M.N., et al. (2024) A state-of-art review on the sustainable technologies for cadmium removal from wastewater. *Water Reuse*, **14**(3), 312–341. <https://doi.org/10.2166/wrd.2024.143>

51. Xu S., Luo X., Huang Q., Chen W. (2021) Calcium-crosslinked alginate-encapsulated bacteria for remediating of cadmium-polluted water and production of CdS nanoparticles. *Appl. Microbiol. Biotechnol.*, **105**(5), 2171-2179. <https://doi.org/10.1007/s00253-021-11155-8>

52. Lee H.K., Choi J.W., Kim J.H., Kim C.R., Choi S.J. (2021) Simultaneous selective removal of cesium and cobalt from water using calcium alginate-zinc ferrocyanide-cyanex 272 composite beads. *Environ. Sci. Poll. Res.*, **28**(31), 42014-42023. <https://doi.org/10.1007/s11356-021-13342-6>